nature communications

Article

https://doi.org/10.1038/s41467-025-60737-x

Intraoperative nerve-specific fluorescence visualization in head and neck surgery: a Phase 1 trial

Received: 15 May 2024

Accepted: 22 May 2025

Published online: 02 July 2025

Check for updates

Yu-Jin Lee[1,8], Ryan K. Orosco[2,8], Michael Bouvet[3], Jeremy D. Richmon[4], Brett J. Berman[5], Kayva L. Crawford[6], Marisa Hom[7], Quyen T. Nguyen[5,6,9] & Eben L. Rosenthal[7,9]

Iatrogenic nerve injury is a surgical complication with significant morbidity. This clinical trial, now complete, investigates the systemic administration of bevonescein, which selectively binds to nerves, in a single-arm, prospective multi-center, dose-escalation Phase 1 trial in adult patients with head and neck neoplasms undergoing parotidectomy or thyroidectomy in the United States. Twenty-seven participants are enrolled in the trial and receive the systemic agent. The primary outcome is safety with no dose-limiting toxicity among the 27 patients, but a single adverse event was identified that was possibly related to the study drug (vomiting). Secondary outcomes include the pharmacokinetics, optimal dose, and timing of bevonescein. The half-life of bevonescein is 29–72 min, and the optimal dose is 500 mg by objective measures, with the fluorescence signal-to-background ratio (SBR; 2.1 ± 0.8) significantly higher compared to white light (1.3 ± 0.2; $p = 0.003$). The fluorescent SBR of nerves between the early (1–3 h) versus late (3–5 h) timing cohorts is not statistically different. Here, we present data of a nerve imaging agent showing that preoperative intravenous infusion of bevonescein is well tolerated. This trial is registered at ClinicalTrials.gov (NCT04420689) and is sponsored by Alume Biosciences (San Diego, CA).

Fluorescence-guided surgery (FGS) is being integrated into surgical practice to improve surgical outcomes. There are several intraoperative fluorescent agents approved for surgical imaging of cancer, and more than a dozen in late-stage trials[1–6]. Unfortunately, targeting nerve tissue has proved more challenging, and there are currently no approved fluorescent agents for nerve visualization. Developing targeted imaging agents to enhance nerve structures for FGS has lagged behind cancer-specific contrast agent development since unique antigens are more difficult to target in normal tissues compared to tumors that overexpress many unique cancer cell-surface antigens.

Improving intraoperative imaging of nerves represents a critical unmet need in surgical practice to prevent nerve injury in the 40 million operations conducted each year in the U.S[7]. Injury to nerves can leave subjects with significant morbidity, including chronic pain, numbness, or paralysis[8]. The impact of injuring even small branches of the facial nerve can result in significant cosmetic and functional quality

[1]Department of Otolaryngology-Head and Neck Surgery, Stanford University, Palo Alto, CA, USA. [2]Department of Surgery, Division of Otolaryngology-Head and Neck Surgery, University of New Mexico, Albuquerque, NM, USA. [3]Department of Surgery, University of California, San Diego, La Jolla, CA, USA. [4]Department of Otolaryngology-Head and Neck Surgery, Mass Eye and Ear, Harvard Medical School, Boston, MA, USA. [5]Alume Biosciences, San Diego, CA, USA. [6]Department of Otolaryngology-Head and Neck Surgery, University of California, San Diego, La Jolla, CA, USA. [7]Department of Otolaryngology-Head and Neck Surgery, Vanderbilt University, Nashville, TN, USA. [8]These authors contributed equally: Yu-Jin Lee, Ryan K. Orosco. [9]These authors jointly supervised this work: Quyen T. Nguyen, Eben L. Rosenthal. e-mail: e.rosenthal@vumc.org

of life challenges, including ocular dryness and difficulty eating[9,10]. Injury to the recurrent laryngeal nerve resulting in vocal fold paralysis occurs during many common procedures, including thyroid surgery, anterior approaches to the cervical spine, and carotid endarterectomy. These significant morbidities associated with iatrogenic nerve injury occur up to 13% in head and neck surgeries[7].

Therefore, improving a surgeon's ability to visually efficiently identify nerves during anatomic dissection is widely recognized to have a huge potential for a paradigm-shift in the field of surgery. In fact, improvements in surgical imaging technology and fluorescence chemistry are bringing several very promising agents to the clinic. Interest in real-time intraoperative fluorescence highlighting of nerves is growing[11,12] because of the obvious clinical application. The field is very new, and approaches to the problem vary between groups. Summers et al. developed a promising near-infrared probe which has the advantages of excellent tissue penetration at the higher wavelength[13,14]. In addition, nonspecific fluorophores, such as indocyanine green alone, have also been reported in clinical studies to improve intraoperative visualization of nerves using near-infrared fluorescence imaging, but this data is has not been widely reported[15,16]. It is very likely that in the near future, surgeons may have several options of imaging agents and devices to assist in the identification of nerves. However, surgeons today must rely on surgical experience and electrophysical stimulation techniques for identification of nerves.

As nerve preservation is a critical component of multiple surgical procedures, multiple nerve imaging agents are under development including NIR oxazines[17,18], GAP-43-Ra-PEG-ICG[19], and HNP401[20]. GAP-43-Ra-PEG-ICG highlights GAP-43 positive neural cells and oxazine-derived dyes are localized to myelin. We developed bevonescein, a small peptide labeled with fluorescein, a fluorophore in the visible range that has been successfully tested in preclinical models[20–24].

Table 1 | Demographics and baseline clinical characteristics

Characteristic		Dose Escalation Cohort (*n* = 15) *n* (%)	Dose Timing Cohort (*n* = 12) *n* (%)	All Cohorts (*n* = 27) *n* (%)
Sex	Female	6 (40)	7 (58)	13 (48)
	Male	9 (60)	5 (42)	14 (52)
Age[a]		54.2 ± 15.9	50.5 ± 20.2	52.6 ± 18.1
Ethnicity	Hispanic or Latino	5 (33)	2 (17)	7 (26)
	Not Hispanic or Latino	10 (67)	9 (75)	19 (70)
	Not reported	0	0	0
	Unknown	0	1 (8)	1 (4)
Race	American Indian or Alaska Native	0	0	0
	Asian	2 (13)	1 (8)	3 (11.1)
	Black or African American	1 (7)	0	1 (3.7)
	Native Hawaiian or Other Pacific Islander	0	0	0
	White	4 (27)	9 (75)	13 (48.1)
	Other	2 (13)	1 (8)	3 (11.1)
	Unknown	6 (40)	1 (8)	7 (25.9)
Surgery Type	Thyroidectomy	3 (20)	1 (8)	4 (14.8)
	Parotidectomy	4 (27)	10 (83)	14 (51.9)
	Neck Dissection	8 (53)	1 (3)	9 (33.3)

[a]Age was characterized as mean ± SD.

The specific binding site of bevonescein is not yet fully understood and is being evaluated with additional studies. We have shown in animal models binding of bevonescein to the structural extracellular matrix component of the nerves, rather than axons or myelin, which allows visualization of both intact and degenerated nerves in preclinical models[25].

We designed this clinical trial for patients at high risk for nerve injury – those undergoing surgical procedures that require identification and preservation of the facial nerve (parotidectomy), recurrent laryngeal nerve (thyroidectomy) and the spinal accessory nerve (neck dissection). Although several promising agents are actively undergoing evaluation, there is currently no agents approved for real-time intraoperative fluorescence highlighting of nerves[26,27]. Here we report the results of a clinical trial evaluating an agent, bevonescein (ALM-488) designed to improve nerve visualization[28].

Results

Clinical trial profile

Of the 27 enrolled patients, 70% were under 65 years of age, 26% were Hispanic or Latino, and 48% were female (Table 1). Parotidectomy was the most common surgical procedure (52%), followed by cervical lymphadenectomy (33%) and thyroidectomy (15%). All patients underwent surgery for neoplastic disease. The first 15 patients were enrolled in the dose-escalation cohort (Cohort A), which was designed as a traditional 3 + 3 study design, where subjects received the study drug in tiers: 100, 200, 400, 500, and 600 mg. Once the optimal dose was identified, 12 additional patients were in enrolled at the optimal dose to determine optimal timing between infusion and surgical incision (Cohort B). In the timing cohort, there were 6 subjects who received the agent 1–3 h prior to surgery start, and 6 subjects who were dosed 3–5 h prior to surgery. A total of 102 unique nerves were identified in the study (Table 2).

Primary Outcome: Safety

The safety profile following intravenous ALM-488 administration was evaluated using multiple metrics including vital signs, physical examination including neurological exam, adverse event monitoring, evaluation for evidence of dose-limiting toxicities (DLT), infusion reactions as well as cardiac monitoring using electrocardiogram (ECG) and clinical laboratory assessments including urinalysis, hematology, chemistry, coagulation markers, biomarkers including histamine, tryptase, C3a, and C5 before, during and after infusion and for 30 (+5) days following infusion.

For all doses tested, no DLTs were reported and there were no infusion reactions. At any dose level including the maximal dose of 600 mg, there were no dose-limiting toxicities (DLTs). Twelve of the 27 (44%) subjects experienced one or more adverse events (AE), with a total of 32 AEs reported (Table 3). Of these AEs, a single AE was assessed as possibly related to the study drug (retching without

Table 2 | Number of unique nerves per cohort

Cohort		Dose/Time (*n* = Subjects)	Total number of unique nerves per cohort
Dose	Cohort 1	100 mg (*n* = 3)	5
	Cohort 2	200 mg (*n* = 3)	11
	Cohort 3	400 mg (*n* = 3)	11
	Cohort 4	600 mg (*n* = 3)	17
		500 mg (*n* = 3)	14
Timing[a]	Cohort 1	1–3 h (*n* = 6)	29
	Cohort 2	3–5 h (*n* = 6)	15
Total		*n* = 27	102

[a]Subjects in the timing cohort received 500 mg of bevonescein.

Table 3 | Adverse events

Cohort	Dose	Age, Sex	Adverse Event	Serious	Relationship to bevonescein	Severity (Grade)	Outcome (as of study completion)
Dose-Defining	100 mg	40 F	Nausea	No	Unlikely related	1	Resolved
			Body aches	No	Unlikely related	1	Resolved
	100 mg	56 F	Chills	No	Unlikely related	1	Resolved
			Non-cardiac chest pain	No	Unrelated	1	Resolved
			Nerve damage (foot)	No	Unrelated	1	Not resolved
			Urinary tract infection	No	Unrelated	1	Not resolved
	200 mg	54 F	Dysphonia	No	Unrelated	1	Resolving
	400 mg	53 M	Left face paresis	No	Unrelated	1	Resolved
			Leg soreness (bilateral)	No	Unrelated	1	Resolved
			Left antecubital skin bruising	No	Unrelated	1	Resolved
			Seroma, surgical site	No	Unrelated	1	Resolved
	600 mg	59 M	Neck Infection, sialoadenitis	Yes	Unrelated	3	Resolved
			COVID-19 infection	No	Unrelated	1	Resolved
			Salivary gland fistula	No	Unrelated	1	Not resolved
	600 mg	54 F	Dry skin (face)	No	Unrelated	1	Resolved
Dose-Timing 1–3 h	500 mg	68 F	Marginal nerve weakness (right)	No	Unrelated	1	Not resolved
			Neck abscess	No	Unrelated	2	Not resolved
		53 F	Facial asymmetry	No	Unrelated	1	Not resolved
			Lower lip weakness (right)	No	Unrelated	1	Not resolved
			Sialocele (parotid)	No	Unrelated	2	Resolved
		21 F	Skin tenderness (incision site)	No	Unrelated	1	Not resolved
			Urinary tract infection	No	Unrelated	1	Resolved
			Numbness (ear lobe, right)	No	Unrelated	1	Not resolved
			Weakness (brow, right)	No	Unrelated	1	Not resolved
Dose-Timing 3–5 h	500 mg	67 F	Preauricular edema	No	Unrelated	1	Resolved
			Dizziness	No	Unrelated	1	Resolved
			Shortness of breath	No	Unrelated	2	Resolved
		66 M	Shoulder pain (bilateral)	No	Unrelated	1	Resolved
			Neck stiffness	No	Unrelated	1	Resolved
			Dental infection (first episode)	Yes	Unrelated	3	Resolved with sequelae
			Dental infection (second episode)	No	Unrelated	2	Resolved
		48 M	Dry heaves	No	Possibly related	1	Resolved

vomiting), which resolved without intervention. Two serious AEs (SAE; dental infection, neck infection) occurred in the 27 subjects (7.4%). Neither of these was considered to be related to the study drug. No patients were discontinued from the study due to AEs. There were no patients who met study stopping or suspension rules. There were no patients who reported IRR or adverse device effects. No deaths were reported during the study.

There were no trends in changes from baseline to any of the timepoints in vital sign parameters in any of the cohorts. The changes from baseline in vital signs were small, and no clinically significant or relevant differences were observed among cohorts. Overall, the majority of patients in all cohorts had normal physical examination findings at all timepoints analyzed, except for the head, eyes, ears, nose, and throat body system. A total of 22 (81.5%) patients reported abnormal results and these were comparable across all treatment cohorts, and none of the abnormalities were reported as an AE. All patients had normal ranges or not clinically significant abnormalities for hematology, chemistry, coagulation, and urinalysis as deemed by the investigators, showed no clinically relevant differences among cohorts, and did not indicate any unexpected safety issues (Table 4).

All patients had normal or non-clinically significant abnormal ECG values, and these were comparable across all cohorts. Overall, the changes from baseline in 12-lead ECG were small, and no clinically significant or relevant differences were observed among the cohorts. Out-of-range histamine values were observed after infusion in 14 of the 27 patients, of which 11 had out-of-range values or values not done at pre-infusion (Table 5). None of the histamine out-of-range values were deemed by the investigators to be clinically significant, and no AEs were reported as a result of out-of-range blood allergy levels. Tryptase and complements C3a and C5 levels remained stable during the study (Table 4).

Secondary outcome: pharmacokinetics

Pharmacokinetics of bevonescein showed the mean half-life ranged from 29 to 72 min (Fig. 1). The mean AUC_{last} values of the bevonescein not bound to plasma or tissue proteins (unbound) increased 6.1-fold over the 6-fold increase in dose suggesting dose proportionality. The mean unbound AUC_{last} values were about 3.3- to 3.5-fold lower than the total bevonescein AUC_{last} values, suggesting that the free fraction was approximately 30%.

https://doi.org/10.1038/s41467-025-60737-x

Table 4 | Quantitative Laboratory Parameters (Hematology, Chemistry, Coagulation, Urinalysis, Blood Allergy Levels) by Cohort

Laboratory Parameter		Dose-defining cohort		Dose-timing cohort	
		Pre-infusion (*n* = 15)	Day 1 (22 hrs post-infusion) (*n* = 15)	Pre-infusion (*n* = 12)	Day 1 (22 hrs post-infusion) (*n* = 11)
Hematology	Erythrocytes (10^{12}/L)	4.5 ± 0.6	4.2 ± 0.6	4.4 ± 0.5	4.2 ± 0.4
	Hemoglobin (g/dL)	13.4 ± 1.6	12.5 ± 1.8	13.2 ± 1.6 = 5	12.6 ± 1.0
	Hematocrit (fraction of 1)	0.4 ± 0.04	0.4 ± 0.05	0.4 ± 0.05	0.4 ± 0.03
	Mean corpuscular volume (fL)	89.3 ± 6.4	89.5 ± 6.8	90.3 ± 3.8	90.1 ± 4.4
	Leukocytes (10^9/L)	6.8 ± 3.0	12.1 ± 3.0	6.4 ± 1.9	11.8 ± 2.8
	Platelets (10^9/L)	263 ± 71	265 ± 76	245 ± 63	242 ± 54
	Neutrophils (10^9/L)	3.8 ± 2.4	9.3 ± 3.2	3.8 ± 1.3	9.3 ± 2.9
	Eosinophils (10^9/L)	0.2 ± 0.1	0.02 ± 0.1	0.2 ± 0.1	0.03 ± 0.1
	Basophils (10^9/L)	0.03 ± 0.04	0.01 ± 0.03	0.04 ± 0.04	0.01 ± 0.3
	Lymphocytes (10^9/L)	2.3 ± 1.3	2.0 ± 1.6	1.9 ± 0.7	1.7 ± 0.9
	Monocytes (10^9/L)	0.5 ± 0.2	0.7 ± 0.2	0.5 ± 0.2	0.7 ± 0.2
Chemistry	Alkaline phosphatase (ukat/L)	1.1 ± 0.4	1.0 ± 0.4	1.3 ± 0.4	1.1 ± 0.3
	Aspartate aminotransferase (ukat/L)	0.4 ± 0.1	0.5 ± 0.2	0.4 ± 0.1	0.3 ± 0.1
	Alanine aminotransferase (ukat/L)	0.4 ± 0.2	0.4 ± 0.2	0.3 ± 0.1	0.3 ± 0.1
	Bilirubin (umol/L)	7.5 ± 2.6	8.4 ± 4.0	7.6 ± 4.8	9.1 ± 5.5
	Calcium (nmol/L)	2.3 ± 0.1	2.2 ± 0.1	2.3 ± 0.1	2.2 ± 0.1
	Phosphate (nmol/L)	1.1 ± 0.2	1.1 ± 0.3	1.1 ± 0.2	1.0 ± 0.2[a]
	Blood urea nitrogen (nmol/L)	5.1 ± 1.6	4.9 ± 1.6	5.3 ± 2.0	4.4 ± 1.3
	Creatinine (umol/L)	77.9 ± 15.6	72.8 ± 15.2	68.4 ± 15.7	66.5 ± 12.8
	GFR	84.6 ± 11.2	83.6 ± 15.0	93.1 ± 19.6	94.0 ± 15.6
	Protein (g/L)	71.9 ± 3.9	68.1 ± 5.8	70.8 ± 4.9	65.4 ± 5.0
	Albumin (g/L)	43.2 ± 4.1	40.3 ± 3.7	43.5 ± 3.2	40.1 ± 3.2
	Glucose (mmol/L)	5.7 ± 0.7	6.7 ± 1.5	6.5 ± 2.8	8.7 ± 5.3
	Potassium (mmol/L)	4.2 ± 0.5	4.0 ± 0.4	4.4 ± 1.1	4.0 ± 0.5
	Sodium (mmol/L)	139.1 ± 1.9	137.5 ± 3.0	138.9 ± 1.6	138.2 ± 2.7
	Chloride (mmol/L)	101.6 ± 2.7	99.6 ± 3.0	103.8 ± 2.5	103.2 ± 3.0
	Magnesium (mmol/L)	0.8 ± 0.1	0.8 ± 0.1	0.9 ± 0.1	0.8 ± 0.1
	Bicarbonate (mmol/L)	25.9 ± 2.8	25.3 ± 3.0	26.0 ± 2.5	25.1 ± 1.9
	Urate (umol/L)	315 ± 66	255 ± 70	292 ± 130	235 ± 104
	Lactate dehydrogenase (ukat/L)	3.7 ± 1.2	3.3 ± 1.1	4.4 ± 2.9	3.1 ± 0.7
Coagulation	Prothrombin time (sec)	12.3 ± 1.0	13.2 ± 1.4	12.8 ± 1.0	13.7 ± 1.3
	Activated partial thromboplastin time (sec)	31.1 ± 2.4	29.7 ± 2.5	33.0 ± 2.5	31.4 ± 3.7
	INR	1.1 ± 0.1	1.1 ± 0.2	1.1 ± 0.1	1.1 ± 0.1
Urinalysis	pH	6.4 ± 0.9	6.2 ± 0.9	6.0 ± 0.9[b]	6.1 ± 1.1[a]
	Specific gravity	1.0 ± 0.01	1.0 ± 0.01	1.0 ± 0.0[b]	1.0 ± 0.004[a]
Blood Allergy Levels	Tryptase	5.4 ± 2.2	4.3 ± 1.4[c]	5.5 ± 2.0	4.3 ± 1.5
	Complement C3a	195 ± 100 [d]	231 ± 153[c]	253 ± 207[e]	241 ± 156
	Complement C5	17.8 ± 3.6 [d]	17.3 ± 6.0 [d]	15.8 ± 5.1[a]	16.8 ± 3.3

All values are represented as mean ± SD
[a]*n* = 10;
[b]*n* = 11;
[c]*n* = 13;
[d]*n* = 12;
[e]*n* = 9

Secondary outcome: optimal dose of bevonescein

In evaluating the secondary endpoint of optimal dose, we found that all doses of bevonescein (100–600 mg) yielded nerve fluorescence intraoperatively with significantly higher SBR in fluorescent (FL) compared to white light reflectance (WLR) images at all doses and across all nerve categories (Fig. 2). At 600 mg there was increased background fluorescence (mean pixel intensity (MPI) 73.2 ± 34, compared to 39.5 ± 17 in the 500 mg cohort; Welch ANOVA $p < 0.01$) which impaired tissue contrast (SBR 2.2 ± 1.6, compared to 3.0 ± 1.0 in the 500 mg cohort; Kruskal-Wallis $p > 0.05$) (Fig. 3). No further dose escalation was pursued beyond 600 mg due to imaging considerations. The 500 mg dose was determined to have optimal improvement in nerve visualization relative to other doses and was therefore chosen as the optimal dose for the timing cohorts (see examples of intraoperative images in Fig. 4 and additional examples in Supplementary Fig. 2).

https://doi.org/10.1038/s41467-025-60737-x

Table 5 | Histamine Values in All Patients (Original Units)

Cohort	Patient ID	Specimen	Units	Normal Range	Pre-infusion	Day 1 (22 h post-infusion)
Dose escalation 100 mg	101–001	Plasma	nmol/L	0–8	Not done	85 (H)
	101–002	Plasma	nmol/L	0–8	<8	Not done
	101–003	Plasma	nmol/L	0–8	<8	Not done
Dose escalation 200 mg	101–005	Plasma	nmol/L	0–8	22 (H)	<8
	101–006	Plasma	nmol/L	0–8	68 (H)	8
	101–007	Plasma	nmol/L	0–8	<8	<8
Dose escalation 400 mg	101–011	Plasma	nmol/L	0–8	12 (H)	36 (H)
	103–004	Whole blood	nmol/L	180–1800	1418	<174 (L)
	103–006	Whole blood	nmol/L	180–1800	384	174 (L)
Dose escalation 600 mg	101–012	Plasma	nmol/L	0–8	19 (H)	14 (H)
	101–013	Plasma	nmol/L	0–8	34 (H)	<8
	102–001	Plasma	ng/mL	0–1.8	1.5	1.5
Dose escalation 500 mg	101–014	Plasma	nmol/L	0–8	8	<8
	103–005	Whole blood	nmol/L	180–1800	1920 (H)	534
	103–008	Whole blood	nmol/L	180–1800	1620	<174 (L)
Dose timing 3–5 h	101–016	Plasma	nmol/L	0–8	33 (H)	<8
	102–004	Plasma	ng/mL	0–1.8	<1.5	1.5
	103–009	Whole blood	nmol/L	180–1800	1894 (H)	<174 (L)
	103–010	Whole blood	nmol/L	180–1800	2624 (H)	2083 (H)
	103–011	Whole blood	nmol/L	180–1800	1264	297
	103–012	Whole blood	nmol/L	180–1800	1608	489
Dose timing 1–3 h	101–015	Plasma	nmol/L	0–8	11 (H)	<8
	101–017	Plasma	nmol/L	0–8	10 (H)	<8
	101–018	Plasma	nmol/L	0–8	Not done	12 (H)
	102–005	Plasma	ng/mL	0–1.8	<1.5	2.3 (H)
	102–007	Plasma	ng/mL	0–1.8	<1.5	1.5
	103–013	Whole blood	nmol/L	180–1800	653	Not done

L below lower limit of normal.
H above upper limit of normal.

Among those who received the 500 mg dose, there were 54 evaluable nerves in 14 subjects. Objective measurements showed the SBR was significantly higher under FL compared to WL (2.1 ± 0.8 vs.1.3 ± 0.1; $p < 0.05$). Subjectively, surgeon evaluations were obtained using the 4-point discrete Likert Visualization Scoring System (VSS) for 14 subjects who received 500 mg bevonescein. All three categories of the VSS (Contrast Enhancement (CE), Length Measurement (LM), and Branching Delineation (BD)), were superior when evaluating the paired FL overlay images compared to the WLR images (Table 6). We found that 78% of individual nerves (n = 42/54) showed improvement in length measurements, and more than a quarter of the nerves had greater than 20% increase in length of the nerves visualized (Table 7). When individual subjects were considered, we found that every subject (100%) had some improvement in visible nerve length, and 57% of subjects showed a >20% improvement in detectable nerve lengths. Surgeon confidence, nerve discrimination, and the value of fluorescent imaging were all improved in about two-thirds of cases on the NERVE Rating Scale (Supplementary Table 3).

Secondary Outcome: optimal time from infusion to surgery

The signal to background ratio was calculated based on images captured during surgery as a prespecified secondary endpoint. The fluorescent SBR of nerves between the early (1–3 h) versus late (3–5 h) timing cohorts were not statistically different (Fig. 5a). The peak SBR intensity was at 350 min from study drug administration to the time the image was captured, although interpretation is confounded by several outliers with high SBRs during this time interval (Fig. 5b). Not surprisingly, larger nerves (≥2 mm in width) appeared to have higher SBR compared to the smaller nerves (<2 mm) during this window of peak intensity (Fig. 5c).

Discussion

This clinical trial of a nerve-targeted fluorescent nerve agent demonstrates objective increase in signal to background ration (SBR 2.08 ± 0.83 in FL vs.1.32 ± 0.15 in WLR; $p < 0.05$) and improvement in subjective surgeon assessment of the nerve contrast (nerve conspicuity/contrast enhancement 3.3 ± 0.6 in FL vs 2.6 ± 0.5 in WLR; $p = 0.001$ and improvement in nerve length in 78% of subjects with FL images). Although the improvement in length measurement between the two groups does not have obvious clinical implications, we chose this parameter as a proxy for determining the directionality of where the nerve is heading, when it is no longer clearly visible on the surface with white light reflectance. This directionality information may be useful to direct the dissection/tracing of the nerve. There were no adverse events greater than grade 1 attributable to the study drug, and no surgical procedures were canceled or delayed as a result of the infusion. The decision for the 500 mg dose was driven by signal intensity and safety. The economics of drug pricing versus production costs are outside the scope of this manuscript.

The optimal dose and timing were identified based on separate cohorts. Since the study did not identify a maximally tolerated dose and the SBR was relatively consistent across all tested doses, the optimal dose was selected based on the mean pixel intensity (MPI). Use of visible dye requires that the intensity of the signal be strong enough

https://doi.org/10.1038/s41467-025-60737-x

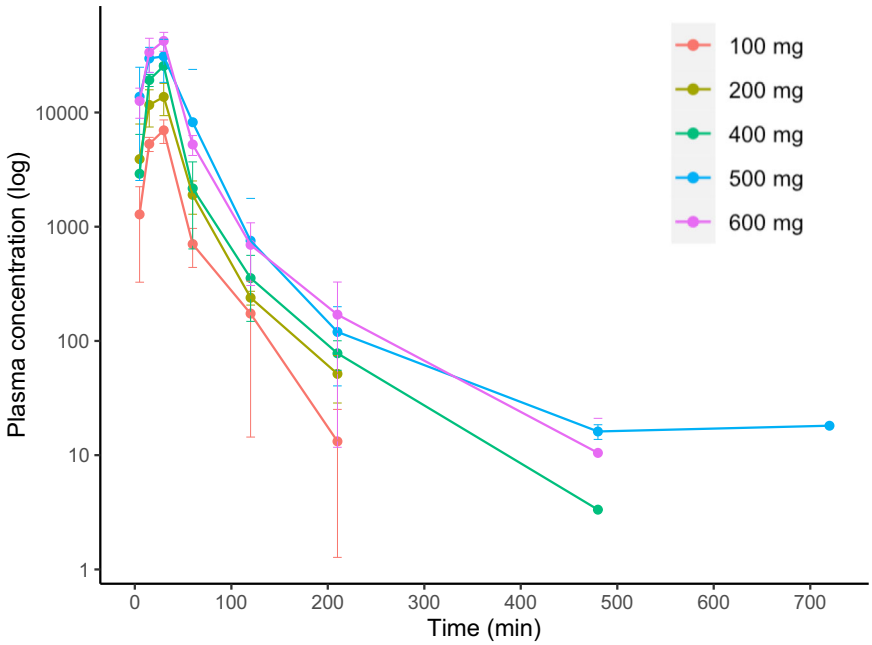

Fig. 1 | Pharmacokinetics of bevonescein (presented in log scale). This demonstrates the dose-dependent pharmacokinetics of bevonescein, consistent with other systematically administered proteins. Detection at levels below 10 ng/mL was not included in the dataset. Each color represents different dose cohorts and error bars represent standard deviation where n ≥ 3. A sample size of the subjects for each dose group was the following: 100 mg, $n = 3$ patients; 200 mg, $n = 3$ patients; 400 mg, $n = 3$ patients; 500 mg, $n = 14$ patients; 600 mg, $n = 3$ patients. The center is defined as the mean. Source data are provided as a Source Data file.

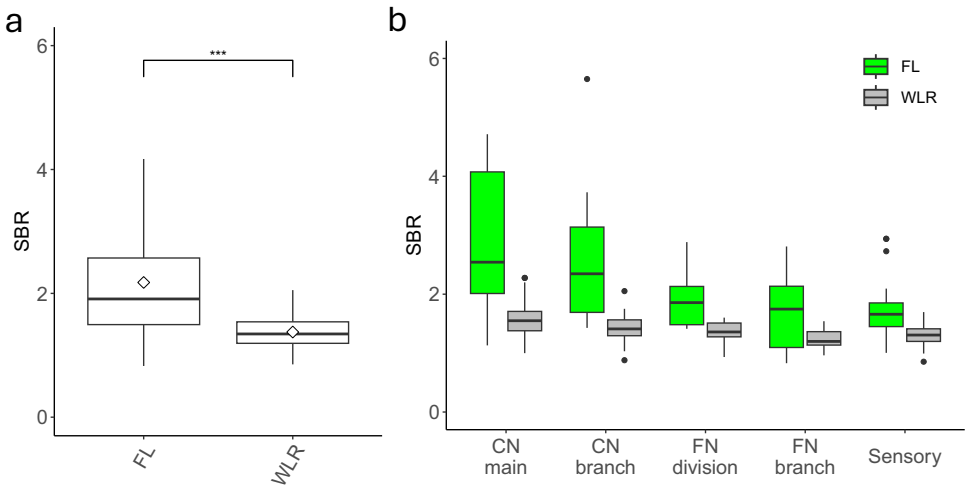

Fig. 2 | Comparison of SBR in WLR and FL images (all cohorts). a The SBR of nerves in FL images was significantly higher ($p < 0.001$) compared to the paired WLR images using two-sided Wilcoxon rank sum test with the sample size $n = 109$ for each group. *** indicates p-value < 0.001. **b** The SBR of FL images were significantly higher compared to the paired WLR images across the nerve categories on a two-sided Wilcoxon rank sum test (p-value < 0.01 for all categories). Adjustments were not made for multiple comparisons. "CN main" includes the facial nerve main trunk, spinal accessory nerve, the hypoglossal nerve, and the vagus nerve ($n = 28$ unique nerves for each FL and WLR). "CN branch" includes recurrent laryngeal nerve and any branches off the main cranial nerve ($n = 17$ unique nerves for each FL and WLR). "FN division" includes the upper and lower divisions of the facial nerve ($n = 13$ unique nerves for each FL and WLR). "FN branch" includes branches from the divisions of the facial nerve, such as the buccal, marginal mandibular branches ($n = 27$ unique nerves for each FL and WLR). "Sensory" includes the greater auricular nerve ($n = 22$ unique nerves for each FL and WLR). Standard boxplots are shown with median as the bold center line, mean as a diamond, the first and third interquartile range (IQR), and the highest and lowest values within 1.5*IQR as hinges, and outliers as additional points. Green represents FL data, and gray represents WLR data. Source data is provided as a Source Data file. SBR signal to background ratio, FL fluorescence, WLR white light reflectance, CN cranial nerve, FN facial nerve.

for visualization with the surgical field especially in the presence of exogenous light sources while minimizing the intensity of the adjacent background tissue. Categorical 4-point discrete Likert evaluation (1–3 h versus 3–5 h) of time from the end of infusion to the first skin incision at the optimal dose of 500 mg did not demonstrate any statistical difference in nerve evaluation between cohorts. When the timing was measured from the end of infusion to when the image was captured, the highest SBR was measured around 300 min (Fig. 5). This highlights the distinction between quantitative SBR measurements and surgeon intraoperative experiences, which may not directly follow

https://doi.org/10.1038/s41467-025-60737-x

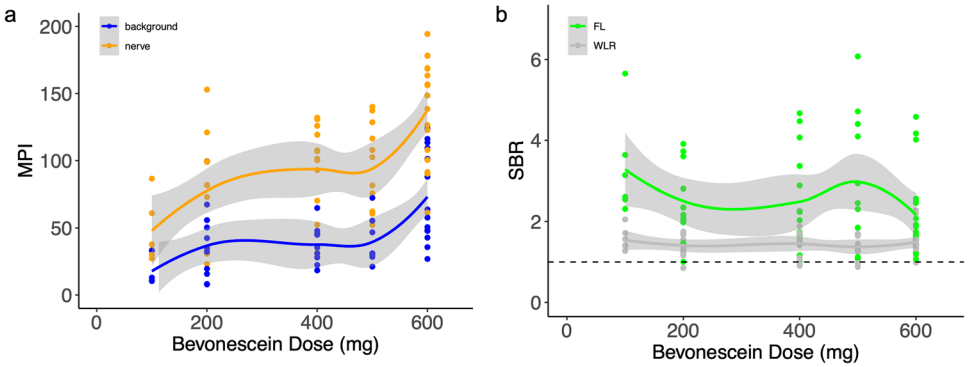

Fig. 3 | The optimal dose of bevonescein is 500 mg. A The MPI of nerves and background in FL images were evaluated, and the background was significantly higher at the 600 mg dose compared to the 500 mg dose. The blue line and dots represent the background MPI, and the orange line and dots represent the nerve MPI. The centers of the lines represent the mean value. The gray shaded error regions represent the standard error. **B** The SBR of FL images at the 600 mg dose decreased compared to the SBR at the 500 mg dose. The green line and dots represent the SBR for FL images and the dark gray line and dots represent the SBR for WLR images. The centers of the lines represent the mean value. The gray shaded error regions represent the standard error. Source data is provided as a Source Data file. MPI – mean pixel intensity; SBR – signal to background ratio; FL – fluorescence; WLR – white light reflectance.

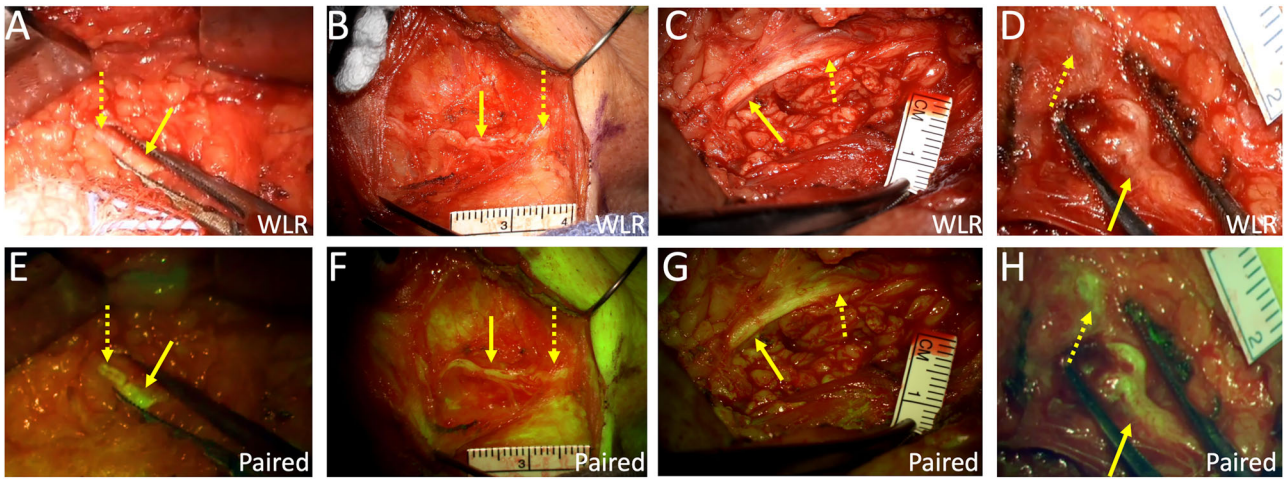

Fig. 4 | Intraoperative nerve images at 500 mg bevonescein dose. Paired intraoperative nerve images from 4 different patients at 500 mg bevonescein dose. WLR images (**A**–**D**) and the same field of view seen with fluorescence signal overlayed on WLR (**E**–**H**). Nerves on the surgical field surface (solid yellow arrows) appear yellowish/green compared to adjacent non-nerve tissue (reddish). There is white surgical gauze visible in the left lower quadrant of **A**. Nerve not on the surgical field surface (dashed yellow arrows) are more easily discernible in **F**, **G**, **H** compared to **B**, **C**, **D**. WLR – white light reflectance; Paired –white light reflectance with fluorescence overlay. The Visualization Scoring System utilized the WLR and Paired images. The SBR analysis utilized the WLR and FL (grayscale) images.

expectations based solely on single time-point quantitative fluorescence measurements.

In order to optimize integration into the surgical workflow, bevonescein was tested using a wide range of time from infusion to skin incision. The data supported a relatively broad timeframe for clinical or subjective visualization (based on nerve conspicuity Contrast Enhancement Score). However, SBR data when measured from still images showed an optimum time of 300 min from infusion to image. In this setting, while SBR can be more precisely measured and quantified, the clinical timing interval was selected for bevonescein-enabled nerve visualization conspicuity. Our experimental design recognized that the study needed to demonstrate improved nerve visualization agent should add quantifiable value to experienced surgeons, rather than to trainees. To this end, only data from attending surgeons are used in the statistical analyses (although trainee data was also collected). Furthermore, to fully delineate the range of the subjective experience, attending surgeons with a range of familiarity with fluorescence-guided surgery were included in the study.

Although this study is the first clinical trial of a targeted nerve agent, non-specific imaging agents have been introduced that have improved nerve visualization. A clinical study of high dose ICG infused the day before surgery utilizing the second window effect improved nerve visualization[29], although these findings are not reported in dozens of published studies using the same dosing protocol to image lung, head and neck, and brain cancers[30–33]. Furthermore, case series evaluating ICG in cranial nerve surgeries (vestibular, trigeminal, vagus schwannomas) showed inconsistent results in highlighting the normal versus tumor tissue with decrease in fluorescence intensity intraoperatively, which can be attributed to the likely lack of neurotropic specificity of ICG[34–36]. ICG is a commonly used fluorophore in FGS applications since it is non-toxic and has unique optical properties, including improved tissue penetration and reduced tissue autofluorescence. Because ICG and other near-infrared dyes (e.g., IRDye800) are outside the visible wavelength on the electromagnetic spectrum, fluorescence can only be visualized using a camera and the images displayed on a screen, adding complexity to the surgical setup.

https://doi.org/10.1038/s41467-025-60737-x

Table 6 | Improved contrast enhancement, length measurement, and branching delineation of 500 mg bevonescein using VSS[a]

	Contrast Enhancement (a.u.)		Length Measurement (mm)		Branching Delineation (a.u.)	
	Per nerve[b] *n* = 55 (mean ± SD)	Per subject[c] *n* = 14 (mean ± SD)	Per nerve *n* = 54[d] (mean ± SD)	Per subject *n* = 14[d] (mean ± SD)	Per nerve *n* = 45[e] (mean ± SD)	Per subject *n* = 10[e] (mean ± SD)
WLR	2.6 ± 0.8	2.6 ± 0.5	358 ± 307	415 ± 403	1.9 ± 0.8	2.0 ± 0.4
Paired FL overlay[f]	3.3 ± 0.8	3.3 ± 0.6	409 ± 368	483 ± 453	2.1 ± 1	2.1 ± 0.4
***p*-value[g]**	0.01	0.001	0.01	0.05	0.01	0.005

[a]The VSS was evaluated by surgeons for 14 subjects in the Phase 1 study, in the following cohorts: dose-escalation (500 mg) *n* = 3, dose-timing (500 mg) *n* = 11.
[b]Per nerve analysis assumes nerves are independent observations.
[c]Per subject analysis uses the mean score of all nerves assessed per subject as the unit of analysis.
[d]Data does not include 1 image from 1 subject in the dose-timing cohort due to errors in device imaging.
[e]Data does not include branching from 1 subject in the dose-escalation cohort and 3 subjects in the dose-timing cohort since the PI denoted there was no branching in these cases.
[f]Fluorescence indicates the use of fluorescence image overlayed on the white light reflectance image.
[g]p-value determined by two-tailed, Student's paired t-test comparing WLR vs paired WLR with FL overlay groups.
VSS Visualization Scoring System, *SD* standard deviation, *WLR* white light reflectance, *FL* fluorescence, *A.u.* arbitrary units, *mm* millimeters.

Table 7 | Improvement of length measurements in subjects receiving 500 mg bevonescein from the VSS

	0% Improvement	Up to 5% improvement	5–10% improvement	11–20% improvement	>20% improvement
Per nerve[a] (*n* = 54)	22% (*n* = 12/54)	18% (*n* = 10/54)	13% (*n* = 7/54)	18% (*n* = 10/54)	28% (*n* = 15/54)
Per subject[b] (*n* = 14)	0 %	14% (*n* = 2/14)	21% (*n* = 3/14)	7% (*n* = 1/14)	57% (*n* = 8/14)

[a]Per nerve analysis assumes nerves are independent observations.
[b]Per subject analysis uses the mean score of all nerves assessed per subject as the unit of analysis.
VSS Visualization Scoring System.
Note: the length measurement component of the VSS was evaluated from images of 14 subjects who received 500 mg of bevonescein in the following cohorts: dose-escalation (*n* = 3), dose-timing (*n* = 11). No statistical adjustments were made if the number of visualized nerves differed per patient.

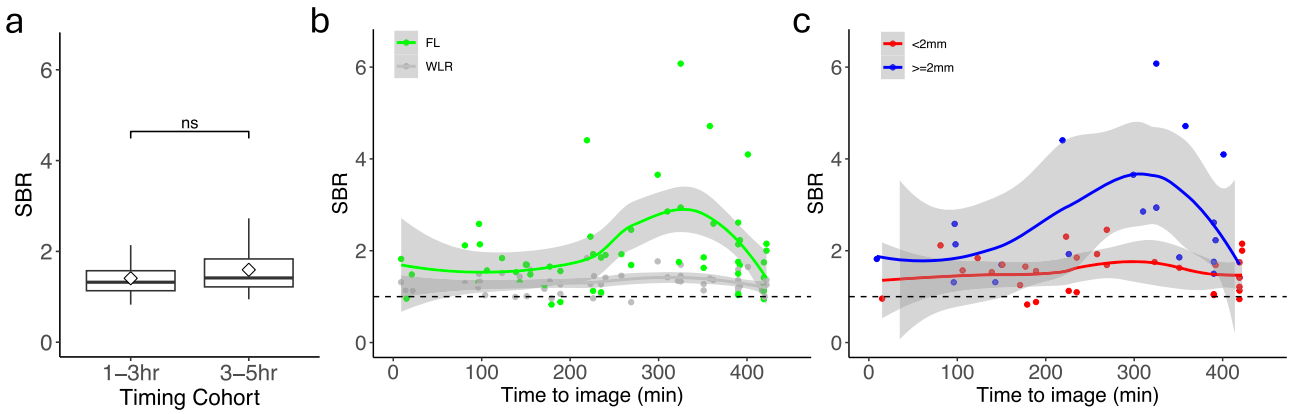

Fig. 5 | Effect of time from infusion to intraoperative imaging on SBR in patients who received 500 mg of bevonescein. a There was no significant difference in SBR of the key nerves when comparing the two timing cohorts: bevonescein administered 1–3 h (n = 36 unique nerves) vs 3–5 h (n = 58 unique nerves) prior to incision. "ns" = not significant using two-sided Wilcoxon rank sum test. Standard boxplots are shown with median as the bold center line, mean as a diamond, the first and third interquartile range (IQR), and the highest and lowest values within 1.5*IQR as hinges, and outliers as additional points. **b** The peak SBR intensity was at 350 min from study drug administration to the time the image was captured. The green line and dots represent the SBR for FL images, and the dark gray line and values represent the SBR for WLR images. The centers of the lines represent the mean value. The gray shaded error regions represent standard error. **c** The effect of time from infusion of 500 mg bevonescein to intraoperative imaging on SBR on nerve width. The presented data included all patients who received the 500 mg dose (including those from the dose-escalation cohort and the dose-timing cohort). The red line and dots represent the SBR for FL images for nerves less than 2 mm, and the blue line and dots represent the SBR for FL images for nerves greater than or equal to 2 mm. The centers of the lines represent the mean value. The gray shaded error regions represent the standard error. Source data is provided as a Source Data file.

Since multiple infrared agents are being developed for intraoperative tumor visualization, we considered it advantageous for a nerve imaging agent to emit in a different spectral range so that dual-imaging (tumor and nerve) would be possible in the same case. Although infrared agents are within the workflow for endoscopic, laparoscopic, robotic, or other minimally invasive techniques, they remain outside the workflow of open surgical procedures. Those agents within the visible wavelength, such as fluorescein (the active fluorophore in bevonescein), can be visualized by the unaided eye with appropriate illumination and filters within the open surgical field. Of

note, visualization with sodium fluorescein alone has also been reported in small case series showing increased fluorescence intensity, in schwannomas, neurofibromas, and spinal cord lesions compared to normal nerve tissue, likely due to accumulation of sodium fluorescein due to abnormal tumor vascular permeability[37–41]. Thus, although these studies highlight the role of fluorescein in targeting abnormal nerve neoplasms, they not address the unmet need of identifying pathologically uninvolved nerves to avoid iatrogenic nerve injury.

Surgeons rely on multiple sensory inputs that are often used in combination to identify and preserve critical structures, especially when the anatomy is distorted by the pathological process that provided the surgical indication. Enhancement of nerves traversing the operative field provides an incremental advantage to the surgeon when integrated with surgical skill, experience, and other sensory inputs. Given the number of factors that contribute to successful nerve preservation, the incremental value of improving nerve visualization is difficult to quantify. Ultimately, these technologies will not be adopted by the surgical community unless they provide clinical benefit and/or increase surgeon confidence. Similarly, evidence that nerve preservation using intraoperative nerve monitoring (IONM) was not documented until it became widely used, in large part because nerve monitoring improved surgeon confidence – a subjective parameter that is difficult to quantify. However, IONM has widespread use and the value of nerve monitoring has been demonstrated now using retrospective studies for thyroid surgery[42–44], parotid surgery[45,46], and a variety of other surgeries throughout the body, although it continues to be controversial[47–50]. Just as nerve monitoring provides additional information during the surgery – improvements in surgical technology can provide complementary data to surgeons to reduce iatrogenic nerve injury. Although many agents are being developed in the NIR range, agents in the visible wavelength support open field surgery and can be used with tumor detection agents that are often in the NIR range. Furthermore, as an imaging agent it is a significant improvement over the current standard of care using electrophysical stimulation, which gradually results in nerve weakness with overstimulation and cannot identify sensory nerves. Perhaps more importantly, the use of a wide field imaging technique, nerve monitoring, and stimulation techniques should provide mutually reinforcing information and could effectively be used to reduce iatrogenic nerve injury, much like the use of MRI, CT, or US, which have their own advantages and limitations. In surgical procedures where microscopic magnification is within the surgical workflow, a surgical microscope with a 560 nm filter can be used to visualize bevonescein. To address wide field procedures, we have ongoing studies to assess the feasibility of surgical loupes that have integrated filters appropriate for bevonescein to be used throughout the surgery.

Intraoperative imaging trials are complicated by the balance of objective and subjective improvements. If the signal-to-noise ratio improves objectively by objective measures, it does not necessarily translate to clinical relevance. On the other hand, subjective improvements in the visualization of nerves is biased and surgeon-dependent. Importantly, we demonstrated a statistically significant difference could be measured in both objective and subjective measurements. A reduction in iatrogenic injury is the ultimate demonstration of benefit, however, the variations in clinical settings and surgical technique will make this challenging to demonstrate. Given the favorable safety profile and encouraging initial results, several multi-institutional Phase 3 studies are currently underway.

Methods

Trial design and oversight

Our prospective open-label Phase 1 trial evaluated the safety and efficacy of bevonescein for intraoperative fluorescence nerve imaging (ClinicalTrials.gov NCT04420689). Bevonescein (ALM-488) is a synthetic peptide of 17 amino acids conjugated to a fluorescein derivative (FAM; 5-carboxyfluorescein) that selectively binds to nerve tissue. The trial was conducted at three academic hospital sites in the United States (Jacobs Medical Center, University of California, San Diego; Stanford Hospital, Stanford University; and Massachusetts Eye and Ear Infirmary, Harvard University). For this study, the three clinical sites were participants of the SMART IRB platform[51]. University of California, San Diego IRB served as the approving institutio,n and the other institutions (Stanford and Mass Eye and Ear) formally ceded approval according to SMART IRB policies.

Investigators from all three sites were required to attend multiple meetings to ensure consistent intraoperative data collection as specified in the protocol. Written informed consent was obtained from all participants, and the study was conducted in adherence with the Declaration of Helsinki. The Study Protocol and the amended Study Protocol are available in Supplementary Information. The study was amended to designate the trial as Phase 1/2 by the FDA, and further clarification of screening labs and follow-up visits.

Inclusion criteria included adults ≥18 years of age with a neoplasm in the head and neck region undergoing head and neck surgery (thyroidectomy, parotidectomy, cervical lymphadenectomy) as part of standard of care treatment. Included subjects had normal liver and renal function, and if of childbearing potential, had a negative urine or serum pregnancy test and were using a medically acceptable form of contraception (e.g., hormonal birth control, intrauterine devices, double-barrier method) or abstinence. If male, the subjects were included if using a medically acceptable form of contraception (e.g,. condom) or abstinence. Exclusion criteria included prior surgery or radiation to the surgical bed, prior chemotherapy, cardiac arrhythmia not controlled with medication, history of stroke within one year, heart failure within past year, history of drug-induced acute tubular necrosis, other investigational drug exposure within past 6 weeks, pregnant or breastfeeding, fluorescein allergy, or severe or steroid dependent asthma.

Following informed written consent at a preoperative encounter, laboratory tests (serum: hematology, coagulation, chemistry, and inflammatory marker panels, pregnancy test (if applicable); urine: urinalysis), electrocardiogram (ECG), and a chest X-ray were obtained.

The study aimed to enroll 21–48 subjects; 9–36 subjects in the dose escalation/de-escalation cohorts and 12 subjects in the dose timing cohort. The dose-defining portion of the study included dose escalation and dose de-escalation cohorts of 3–6 patients per cohort. The dose-escalation tiers included potential doses of 100–100 mg. The dose de-escalation tiers included potential doses of 12.5–50 mg. We initiated the study with a dose of 100 mg based on FDA guidance and non-clinical toxicology studies. Progression to the next dose tier was contingent on safety in three subjects, without DLT, with the option to enroll three additional subjects at any given tier, if needed. Safety and efficacy review of each cohort was completed before progressing to the next cohort. Five doses (100 mg, 200 mg, 400 mg, 500 mg, 600 mg) with 3 subjects at each dose were evaluated with a total of 15 subjects. No safety-related concerns were identified at any dose tested. The 500 mg dose was identified as optimal for safety and efficacy and was chosen for progression to the dose-timing portion of the study. A total of 15 subjects were accrued to the dose-defining cohorts.

Dose-timing cohorts used the optimal imaging dose to compare administration at 1–3 h versus 3–5 h before surgery. Six subjects were enrolled in each cohort. A total of 12 subjects were accrued to the dose-defining cohorts.

The total study was 27 subjects (15 subjects in the dose-defining cohorts +12 subjects in the dose-timing cohorts). Subjects received a single dose of bevonescein via intravenous infusion over 30 min on Day 1. Lab tests and ECG were repeated on Day 1 prior to administration of the study agent and at the end of infusion. For safety monitoring, subjects remained on-site for at least 23-h after dosing. Safety assessments, including adverse events (AEs), and clinical laboratory

tests were performed at Day 1, Day 15 (±8 days), and Day 28 (+5 days). A follow-up visit and lab tests were performed on Day 15 (+/−7 days), and an end-of-trial encounter and laboratory tests on Day 28 (+5 days). Participants were compensated with $50 at each visit, up to four total visits.

The first participant's first visit date was 6/18/2020, and the last participant's last visit date was 6/25/2021.

Intraoperative imaging

The operating surgeon conducted the initial phases of the operation, including nerve dissection and exposure consistent with the surgeon's preference. Per FDA guidelines to maintain the standard of care, once a nerve is within the surgical field, or is expected to be within the surgical field, the microscope with fluorescence capability (Carl Zeiss Tivato surgical microscope with Meditec AG yellow 560 FL Module) was brought in and was used to obtain white light reflectance (WLR) and fluorescent (FL) images during the surgery pertaining to important steps of the surgical dissection and identification of key nerves. Index nerves were defined for each surgery type – parotidectomy: facial nerve branches (frontal, zygomatic, buccal, mandibular); thyroidectomy (recurrent laryngeal nerve); cervical lymphadenectomy (mandibular branch of the facial nerve, vagus nerve, spinal accessory nerve, hypoglossal nerve) (Supplementary Fig. 1. CONSORT Flow Diagram).

To standardize the image capture, the surgeons were instructed to place the camera at a distance of 200 mm, and directly positioning the camera over the surgical field. To minimize the impact of exogenous light sources, the surgeons were instructed to ambient turn off room lights were turned off and the overhead, and ensure that spot lights were turned directed away from the surgical field, and window shades (if applicable) to be in the down position or were closed, whenever possible during image capture. The superimposition of fluorescence was in real time and through the microscope oculars. Thus, the operating surgeon, via the handgrip controller, was able to toggle back and forth between white light alone, vs. white light with fluorescence overlay to see nerves either with white light reflectance alone (WLR) or white light paired with fluorescence overlay (paired).

Outcomes

The primary objective of the Phase 1 study was to evaluate the safety of bevonescein administered by intravenous infusion by assessing the dose-limiting toxicity (DLT) according to the National Cancer Institute (NCI) Common Terminology Criteria for Adverse Events (CTCAE). Subjects had safety assessments (including clinical laboratory tests and assessment for AEs) on day 1 (day of surgery), day 15 (+−8 days), and day 28 (+−5 days). Secondary objectives were to characterize the pharmacokinetics, determine the dose needed to generate optimal nerve fluorescence, and evaluate the timing of administration. Serum pharmacokinetic (PK) samples were taken on Day 1 pre-dose and at 5, 15, and 30 min, and 1, 2, 3, 8, 12, and 22-h.

Exploratory outcomes: quantitative image analysis

Signal-to-background ratios (SBRs) of the identified nerves in the WLR and FL images were used as a standardized measure to compare across images and subjects, with the background as adjacent non-nerve tissue. All images were reviewed by the team performing image analysis, and optimal images with key indicator nerves per procedure were selected for annotation and analysis. All images were imported into ImageJ, and there was no manipulation of the raw image. For WLR images, the overlay image was used as the raw image. For FL images, the image was split into RGB channels, and the green channel image was used for analysis. For each visualized nerve and adjacent tissue, 5–20 ellipsoid regions of interests were drawn within each tissue. Using a known distance in each image (visible ruler within the operative field and image), the images were set to scale, and the length of the nerves were then measured. The pixel intensities were measured for each region of interest, and the mean of each tissue was then calculated, and background subtraction was performed. The SBR was then calculated by dividing the mean pixel intensity of the nerve by the mean pixel intensity of the background within each image.

Exploratory outcomes: qualitative image analysis

Surgeon questionnaires were utilized—Surgical Imaging Worksheet (SIW) (Supplementary Table 1), Visualization Scoring System (VSS) (Supplementary Table 2), NERVE rating scale (Supplementary Table 3). The VSS scale was developed with the goal of standardizing a clinically relevant rubric to objectively and reproducibly assess surgeon experience in WLR and FL conditions (The VSS included assessments of: Contrast Enhancement (CE) as None, Weak, Clear, Clear or Bright; Length Measurement (LM), in millimeters; and Branching Delineation (BD) as None, Poorly visible, Sufficiently visible, or Excellent visibility). All VSS assessments are done by the operating surgeon at the time of surgery by visualizing the field through the microscopic oculars.

Statistical Analysis

For this Phase 1 study, no formal power calculations were performed. The sample size was determined to be consistent with other studies to meet study objectives. The design of this trial was based on a dose-escalation schema with 3–6 subjects at each tier. The dose tiers were based upon pre-clinical safety data and practical considerations and were designed with input from the FDA, not on a formal statistical power calculation. Safety, clinical, pharmacokinetic, and exploratory outcomes were summarized according to dose with the use of descriptive statistics. Standard boxplots with median as the bold center line, mean as diamond, the first and third interquartile range (IQR), and the highest and lowest values within 1.5*IQR as hinges, and outliers as additional points. The Wilcoxon rank sum test was used to compare the means of the SBRs between FL and WLR images. The optimal dose was determined by evaluating the mean pixel intensity (MPI) of the identified nerves and background of adjacent non-nerve tissue on both FL and WLR images as well as evaluating the SBRs. For normally distributed data with homogeneous variances, ANOVA was used to compare the MPIs of the nerve; for normally distributed data with non-homogeneous variance, Welch ANOVA was used to compare the MPI of the background; and for non-normally distributed data, Kruskal-Wallis was used to compare the SBRs. Post-hoc testing was performed using the Tukey method with the caveat of small sample size and multiple testing in this preliminary study. Scatterplots with trend lines applied with locally estimated scatterplot smoothing (LOESS) and standard errors in gray were used for visualization. Data from the VSS and the NERVE questionnaire were analyzed using the Student's t-test and paired 2-tailed statistical tests as appropriate. All statistical analysis was performed using R (version 4.4.2) and RStudio (version 2024.12.0 + 467).

The parent peptide sequence, from which bevonescein (ALM-488) was derived, was initially identified by phage display using an m13 phage library. Bevonescein and ALM-488 (referenced in the study protocol) are synonymous – ALM-488 is the internal name for the drug prior to the United States Adopted Names (USAN) Council designation. To optimize and determine the core binding domain of the parent peptide, a binding analysis assessment was conducted after systematic deletion of two amino acids from the C or N terminus (Hingorani et al. 2018). Bevonescein is a variant of the parent peptide, with removal of 2 amino acids from the N terminus. An assessment was conducted to compare versions of bevonescein with FAM attached to the C terminus versus the N terminus, which determined that FAM attached to the N terminus demonstrated the highest intensity (Hingorani et al, Theranostics 2018). No difference in toxicity was noted between the different versions of the peptide sequences from which bevonescein was

derived. Based on this data, the version of bevonescein used in the clinical trial described here has FAM attached to the N terminus.

Reporting summary

Further information on research design is available in the Nature Portfolio Reporting Summary linked to this article.

Data availability

The data in this study that underlie the results after deidentification is available in the Source Data file. Data will be made available to investigators whose proposed use of the data has been approved by an independent review committee identified for this purpose to achieve the aims of the proposal. The study protocol is available in the Supplementary Information. Proposals may be after article publication by submitting a proposal to clinical.trial@alumebiosciences.com with a response time of 5–10 business days. To gain access, data requestors will need to sign a data access agreement. Source data are provided with this paper.

References

1. Lee, Y. J. et al. Intraoperative fluorescence-guided surgery in head and neck squamous cell carcinoma. *Laryngoscope* **131**, 529–534 (2021).
2. Ottolino-Perry, K. et al. Intraoperative fluorescence imaging with aminolevulinic acid detects grossly occult breast cancer: a phase II randomized controlled trial. *Breast Cancer Res. BCR* **23**, 72 (2021).
3. Sibinga et al. Intraoperative molecular fluorescence imaging of pancreatic cancer by targeting vascular endothelial growth factor: a multicenter feasibility dose-escalation study. *J. Nucl. Med. Publ. Soc. Nucl. Med.* **64**, 82–89 (2023).
4. Stibbe, J. A. et al. First-in-patient study of OTL78 for intraoperative fluorescence imaging of prostate-specific membrane antigen-positive prostate cancer: a single-arm, phase 2a, feasibility trial. *Lancet Oncol.* **24**, 457–467 (2023).
5. de Valk, K. S. et al. Dose-finding study of a CEA-targeting agent, SGM-101, for intraoperative fluorescence imaging of colorectal cancer. *Ann. Surg. Oncol.* **28**, 1832–1844 (2021).
6. Zapardiel, I. et al. Utility of intraoperative fluorescence imaging in gynecologic surgery: systematic review and consensus statement. *Ann. Surg. Oncol.* **28**, 3266–3278 (2021).
7. Gibbs-Strauss, S. L. et al. Nerve-highlighting fluorescent contrast agents for image-guided surgery. *Mol. Imaging* **10**, 91–101 (2011).
8. Burke, S. & Shorten, G. D. When pain after surgery doesn't go away. *Biochem. Soc. Trans.* **37**, 318–322 (2009).
9. Gaillard, C., Périé, S., Susini, B. & St Guily, J. L. Facial nerve dysfunction after parotidectomy: the role of local factors. *Laryngoscope* **115**, 287–291 (2005).
10. Lee Witt, R. Comparing the long-term outcome of immediate postoperative facial nerve dysfunction and vocal fold immobility after parotid and thyroid surgery. *J. Voice. J. Voice Found.* **20**, 461–465 (2006).
11. Sharp, E. et al. The most commonly injured nerves at surgery: A comprehensive review. *Clin. Anat. N. Y. N.* **34**, 244–262 (2021).
12. Wang, L. G. & Gibbs, S. L. Improving precision surgery: A review of current intraoperative nerve tissue fluorescence imaging. *Curr. Opin. Chem. Biol.* **76**, 102361 (2023).
13. Barth, C. W. et al. Clinically translatable formulation strategies for systemic administration of nerve-specific probes. *Adv. Ther.* **4**, 2100002 (2021).
14. Wang, L. G. et al. Near-infrared nerve-binding fluorophores for buried nerve tissue imaging. *Sci. Transl. Med.* **12**, 542 (2020).
15. Qu, Q. et al. Visualisation of pelvic autonomic nerves using NIR-II fluorescence imaging. *Eur. J. Nucl. Med. Mol. Imaging* **49**, 4752–4754 (2022).
16. He, K. et al. Near-infrared Intraoperative Imaging of Thoracic Sympathetic Nerves: From Preclinical Study to Clinical Trial. *Theranostics* **8**, 304–313 (2018).
17. Wang, L. G., Barth, C. W., Combs, J. R., Montaño, A. R. & Gibbs, S. L. Investigation of Oxazine and Rhodamine derivatives as peripheral nerve tissue targeting contrast agent for in vivo fluorescence imaging. *Proc. SPIE- Int. Soc. Opt. Eng.* **10862**, 108620H (2019).
18. Barth, C. W. & Gibbs, S. L. Visualizing Oxazine 4 nerve-specific fluorescence ex vivo in frozen tissue sections. *Proc. SPIE- Int. Soc. Opt. Eng.* **9696**, 96960R (2016).
19. Lu, W. L. et al. GAP-43 targeted indocyanine green-loaded near-infrared fluorescent probe for real-time mapping of perineural invasion lesions in pancreatic cancer in vivo. *Nanomed. Nanotechnol. Biol. Med.* **50**, 102671 (2023).
20. Hingorani, D. V. et al. Nerve-targeted probes for fluorescence-guided intraoperative imaging. *Theranostics* **8**, 4226–4237 (2018).
21. Wu, A. P. et al. Improved facial nerve identification with novel fluorescently labeled probe. *Laryngoscope* **121**, 805–810 (2011).
22. Hussain, T., Nguyen, L. T., Whitney, M., Hasselmann, J. & Nguyen, Q. T. Improved facial nerve identification during parotidectomy with fluorescently labeled peptide. *Laryngoscope* **126**, 2711–2717 (2016).
23. Hussain, T. et al. Fluorescently labeled peptide increases identification of degenerated facial nerve branches during surgery and improves functional outcome. *PloS One* **10**, e0119600 (2015).
24. Whitney, M. A. et al. Fluorescent peptides highlight peripheral nerves during surgery in mice. *Nat. Biotechnol.* **29**, 352–356 (2011).
25. Crawford, K. L. et al. Identification of degenerated murine facial nerves with fluorescence labeling after transection injury. *Otolaryngol. -Head. Neck Surg. J. Am. Acad. Otolaryngol. -Head. Neck Surg.* **169**, 234–242 (2023).
26. Park, M. H. et al. Prototype nerve-specific near-infrared fluorophores. *Theranostics* **4**, 823–833 (2014).
27. Walsh, E. M. et al. Fluorescence imaging of nerves during surgery. *Ann. Surg.* **270**, 69–76 (2019).
28. Crawford, K. L. et al. A scoping review of ongoing fluorescence-guided surgery clinical trials in Otolaryngology. *Laryngoscope* **132**, 36–44 (2022).
29. He, K. et al. Intraoperative near-infrared fluorescence imaging can identify pelvic nerves in patients with cervical cancer in real time during radical hysterectomy. *Eur. J. Nucl. Med. Mol. Imaging* **49**, 2929–2937 (2022).
30. Jeon, J. W. et al. Near-infrared optical contrast of skull base tumors during endoscopic endonasal surgery. *Oper. Neurosurg.* **17**, 32–42 (2019).
31. De Ravin, E. et al. Indocyanine green fluorescence-guided surgery in head and neck cancer: A systematic review. *Am. J. Otolaryngol.* **43**, 103570 (2022).
32. Stubbs, V. C. et al. Intraoperative imaging with second window Indocyanine green for head and neck lesions and regional metastasis. *Otolaryngol. -Head. Neck Surg. J. Am. Acad. Otolaryngol. -Head. Neck Surg.* **161**, 539–542 (2019).
33. Teng, C. W. et al. Second window ICG predicts gross-total resection and progression-free survival during brain metastasis surgery. *J. Neurosurg.* **135**, 1026–1035 (2021).
34. Peng, K. A. & Lekovic, G. P. Intraoperative fluorescence with second window indocyanine green enhances visualization during vestibular schwannoma surgery. *Otol. Neurotol.* **43**, e259–e262 (2022).
35. Schäfer, B. et al. Technique and expected benefit of intraoperative perfusion imaging of peripheral nerves. *Plast. Reconstr. Surg. Glob. Open* **12**, e6281 (2024).
36. Muhammad, N., Ajmera, S. & Lee, J. Y. K. Intraoperative visualization of cranial nerve schwannomas using second-window indocyanine green: A case series. *Clin. Neurol. Neurosurg.* **240**, 108241 (2024).

37. Vetrano, I. G. et al. Fluorescein-guided removal of peripheral nerve sheath tumors: a preliminary analysis of 20 cases. *J. Neurosurg.* **134**, 260–269 (2019).
38. Pedro, M. T. et al. Sodium Fluorescein as intraoperative visualization tool during peripheral nerve biopsies. *World Neurosurg.* **133**, e513–e521 (2020).
39. Kalamarides, M., Bernat, I. & Peyre, M. Extracapsular dissection in peripheral nerve schwannoma surgery using bright light and fluorescein sodium visualization: case series. *Acta Neurochir.* **161**, 2447–2452 (2019).
40. Chan, S. A. et al. Fluorescein-assisted microsurgical resection of vestibular Schwannoma: A prospective feasibility study. *Otol. Neurotol. Publ. Am. Otol. Soc. Am. Neurotol. Soc. Eur. Acad. Otol. Neurotol.* **43**, 1240–1244 (2022).
41. Ung, T. H., Serva, S., Chatain, G. P., Witt, J. P. & Finn, M. Application of sodium fluorescein for spinal cord lesions: intraoperative localization for tissue biopsy and surgical resection. *Neurosurg. Rev.* **45**, 1563–1569 (2022).
42. Kim, J. et al. Intraoperative nerve monitoring is associated with a lower risk of recurrent laryngeal nerve injury: A national analysis of 17,610 patients. *Am. J. Surg.* **221**, 472–477 (2021).
43. Bai, B. & Chen, W. Protective Effects of Intraoperative Nerve Monitoring (IONM) for Recurrent Laryngeal Nerve Injury in Thyroidectomy: Meta-analysis. *Sci. Rep.* **8**, 7761 (2018).
44. Vasileiadis, I. et al. Association of intraoperative neuromonitoring with reduced recurrent laryngeal nerve injury in patients undergoing total thyroidectomy. *JAMA Otolaryngol. - Head. Neck Surg.* **142**, 994–1001 (2016).
45. Savvas, E. et al. Association between facial nerve monitoring with postoperative facial paralysis in Parotidectomy. *JAMA Otolaryngol. - Head. Neck Surg.* **142**, 828–833 (2016).
46. Chiesa-Estomba, C. M. et al. Facial nerve monitoring during parotid gland surgery: a systematic review and meta-analysis. *Eur. Arch. Oto-Rhino-Laryngol. J. Eur. Fed. Oto-Rhino-Laryngol. Soc. EUFOS Affil. Ger. Soc. Oto-Rhino-Laryngol. - Head. Neck Surg.* **278**, 933–943 (2021).
47. Chung, T. K. et al. Examining national outcomes after thyroidectomy with nerve monitoring. *J. Am. Coll. Surg.* **219**, 765–770 (2014).
48. Still, G. P., Pfau, Z. J., Cordoba, A. & Jupiter, D. C. Intraoperative nerve monitoring for tarsal tunnel decompression: a surgical technique to improve outcomes. *J. Foot Ankle Surg. Publ. Am. Coll. Foot Ankle Surg.* **58**, 1203–1209 (2019).
49. Strommen, J. A., Skinner, S. & Crum, B. A. Neurophysiology during peripheral nerve surgery. *Handb. Clin. Neurol.* **186**, 295–318 (2022).
50. Patel, M. S., Wilent, W. B., Gutman, M. J. & Abboud, J. A. Incidence of peripheral nerve injury in revision total shoulder arthroplasty: an intraoperative nerve monitoring study. *J. Shoulder Elb. Surg.* **30**, 1603–1612 (2021).
51. Cobb, N. et al. The SMART IRB platform: A national resource for IRB review for multisite studies. *J. Clin. Transl. Sci.* **3**, 129–139 (2019).

Acknowledgements

The authors would also like to acknowledge the patients and surgeons who participated in this trial, including Davud Sirjani, MD. Raw data collection was performed by the individual clinical study sites (UCSD, Stanford, Mass Eye & Ear) and aggregated by Cadyia (formerly Clinipace), a contract research organization. Data analyses were performed by Summit Analytical, Inc. Alume Biosciences, Inc provided study funding and drug supply and had a review role in study design. The sponsor did not participate in data collection and analysis. Contributions to the manuscript writing are detailed in the Author Contribution section.

Author contributions

Y.J.L. and R.O. contributed equally to the work, and the manuscript was written by the authors, with the co-first authors, including data collection, data analysis, visualization, writing, and editing. M.B. and J.R. contributed to the manuscript with data collection, methodology, and editing. B.J.B. contributed to the manuscript with data curation, project administration, funding acquisition, and editing. K.L.C. and M.H. contributed to the manuscript with data collection, data analysis, visualization, and editing. Q.T.N. and E.L.R. contributed equally as supervisors to the work and were involved with conceptualization, methodology, analysis, writing, and editing.

Competing interests

Q.T.N. is a co-founder and interim-CEO of Alume. B.J.B. is a co-founder and Chief Medical Officer of Alume. A patent for the technology described in this manuscript has been filed with the United States Patent and Trademark Office (USPTO) by The Regents of the University of California (Q.T.N. and B.J.B.). The other authors declare no competing interests.

Additional information

Supplementary information The online version contains supplementary material available at https://doi.org/10.1038/s41467-025-60737-x.

Correspondence and requests for materials should be addressed to Eben L. Rosenthal.

Peer review information *Nature Communications* thanks Jacqueline Birks, Rutger-Jan Swijnenburg, Adam Mamelak, and the other anonymous reviewer(s) for their contribution to the peer review of this work. A peer review file is available.